PHYSICAL REVIEW B VOLUME 47, NUMBER 15 15 APRIL 1993-I

First-principles study of the structural and electronic properties of Cu clusters

Koblar A. Jackson
Department of Physics, Central Michigan University, Mt. Pleasant, Michigan 48859
(Received 4 August 1992)

The structural and electronic properties of small ($n \leq 5$) Cu clusters are determined from first-principles calculations based on the local-spin-density approximation, using an all-electron, Gaussian-orbital formalism. The computational method includes use of a systematically refined numerical integration mesh, providing extremely accurate total energies and atomic forces, and a variational technique for treating accidental degeneracies at the Fermi level. Equilibrium geometries have been determined for the neutral clusters for $n \leq 5$, as well as for the Cu_2 and Cu_3 anions. The calculated properties of the dimer and trimer structures are examined in detail and compared to existing experimental measurements. The influence of the Cu $3d$ states on cluster properties is analyzed. It is shown that there is significant hybridization between the $3d$ and $4s$ in the cluster bonding states. One effect of this hybridization is a strong bond-length preference in the clusters.

I. INTRODUCTION

There has been tremendous interest recently in the properties of small atomic clusters.[1] Small clusters generally have properties quite distinct from the corresponding bulk materials. These properties are very sensitive to the number of atoms in small clusters, often changing dramatically with the addition or removal of a single atom from the cluster. In larger clusters this size sensitivity is diminished as the clusters become increasingly bulklike. There is considerable interest in charting the evolution of cluster properties as a function of cluster size, in order to better understand the bonding and electronic properties of bulk solids. At the same time, the particular properties of individual small clusters are of fundamental and technological interest.

The electronic structure of transition-metal atoms makes transition-metal clusters particularly interesting. The atoms include both relatively localized $3d$ electrons and relatively delocalized $4s$ electrons. Because of their characteristically different length scales, it can be expected that the $3d$ and $4s$ electronic states will have a very different cluster size dependence. With the atomic structure $3d^{10}4s$, Cu is of special interest. Like the simple alkali-metal atoms, Cu has a single s electron outside a closed-shell electronic configuration. However, the Cu $3d$ states lie close below the $4s$ states in energy, and these d states can thus be expected to play a role in determining the properties of Cu clusters. In the bulk metal, for example, the $3d$ states make a significant contribution to the density of states at the Fermi level,[2] making the electrical conductivity of Cu roughly four times that of K.[3] The influence of the $3d$ electrons is also reflected in the bulk lattice structure. Bulk Cu has the fcc structure, while the alkali metals have bcc ground states.

Cu clusters have received a great deal of attention in the past. Detailed experimental studies of the electronic properties of small Cu clusters have been performed.[4,5] Cluster-size effects on the electronic bands in Cu clusters have also been investigated.[6]

Several theoretical calculations have been carried out on Cu clusters. Quantum chemical methods[7,8] have generally been limited to the smallest cluster sizes. Local-density-functional methods have been used[9] to study selected cluster geometries for a variety of cluster sizes. Most recently, the effective-medium theory, an approximate total-energy method, has been used to investigate the geometries of Cu clusters containing up to 29 atoms,[10] and to compare icosahedral versus cuboctahedral structures for Cu clusters of up to 10 000 atoms.[11]

In this work we use first-principles calculations based on the local-spin-density approximation[12] (LSDA) to determine the ground-state properties of small Cu clusters, with $n \leq 5$. These clusters are small enough that ground-state structures can be found, and their properties systematically studied. The LSDA is known to give highly accurate results for the structural properties of materials,[13] yielding bond lengths, for example, in close agreement with experiment. To investigate the role of the Cu $3d$ electrons in determining the structural and electronic properties of the clusters, we compare and contrast the minimum-energy structures calculated for the Cu clusters with the corresponding alkali-metal clusters. In addition, we analyze the electronic structure of the various clusters to determine the $3d$ character of the bonding states in the cluster.

In the next section we briefly discuss the computational formalism we use to study finite atomic clusters. We then proceed in Sec. III to discuss the results of our calculations for Cu clusters. We present equilibrium geometries for all the neutral clusters with $n \leq 5$. We then discuss the properties of the dimer and trimer in detail, comparing the calculated results with recent experimental measurements, and with results of previous quantum chemical calculations. Next we use recently developed gradient corrections to the LSDA (Ref. 14) to determine molecular binding energies for the clusters. It is shown that the gradient corrections are essential for obtaining binding energies in reasonable agreement with experiment. The

paper concludes with a discussion of the role of the Cu $3d$ states in establising cluster properties.

II. COMPUTATIONAL FORMALISM

The local-spin-density approximation[12] (LSDA) is an accurate first-principles, quantum-mechanical technique for studying the properties of an N-electron system. Extensive applications of the LSDA in the literature demonstrate that structural properties such as bond lengths and vibrational frequencies are given very accurately by the theory, typically within a few percent of the corresponding experimental measurements.[13]

In the LSDA, the ground-state energy of a system of electrons and nuclei is expressed as a function of the nuclear coordinates, $\mathbf{R}_i$, and a functional of the electronic density, ρ:

$$E[\rho]=\sum_{i\le j}\frac{Z_iZ_j}{|\mathbf{R}_i-\mathbf{R}_j|}+\sum_i f_i\langle\psi_i|-\nabla^2/2+V_{\rm nuc}|\psi_i\rangle + \frac{1}{2}\int d\mathbf{r}d\mathbf{r}'\frac{\rho(\mathbf{r})\rho(\mathbf{r}')}{|\mathbf{r}-\mathbf{r}'|}+E_{\rm xc}[\rho(\mathbf{r})]\ , \tag{1}$$

where

$$\rho=\sum_i f_i|\psi_i|^2 \tag{2}$$

and

$$V_{\rm nuc}(\mathbf{r})=-\sum_i\frac{Z_i}{|\mathbf{r}-\mathbf{R}_i|}\ . \tag{3}$$

The various terms in the energy functional represent the internuclear Coulomb interaction, the electron kinetic energy, the electron-nuclear interaction, the classical Coulomb energy of the electrons, and in the last term, the quantum-mechanical exchange-correlation energy, for which we use the Perdew and Zunger parametrization[15] of the Ceperley-Alder electron-gas data.[16] The density is expressed in terms of a set of one-electron orbitals, ψ_i, with occupation numbers $0<f_i<1$. Variation of $E[\rho]$ with resect to the ψ_i's leads to the Kohn-Sham equations, effective Schrödinger equations which must be solved self-consistently for the ψ_i's. Equation (1) has been written in a spin-unpolarized form for convenience. The corresponding spin-polarized expression is a straightforward extension, and is not given here.

Our computer codes implement the LSDA using an all-electron linear-combination-of-atomic-orbitals (LCAO) technique with Gaussian-based orbitals.[17,18] A high degree of accuracy is achieved in the calculations through the use of a numerical integration mesh[17] to evaluate the multicenter integrals required for solving the Kohn-Sham equations and for evaluating the total energy. The mesh can be systematically refined to yield essentially arbitrary accuracy in evaluating the necessary integrals. In the calculations described here, the mesh was typically refined to integrate the total electronic charge of a given cluster to a tolerance of better than $0.001e$, which we find to correspond approximately to an absolute accuracy of 0.001 a.u. (0.027 eV) in integrating the total energy. This level of accuracy was adequate to reliably determine minimum-energy structures in most cases.

To determine the structural properties of the clusters, the total energy is studied as a function of the nuclear coordinates. To do this efficiently, we use the self-consistent electronic orbitals to calculate atomic forces.[18] The forces are simply the gradients of the LSDA total energy with respect to the nuclear coordinates. We include the Pulay correction[19] in our expression for the forces, to account for the dependence of our basis set on the nuclear coordinates. Highly accurate forces are obtained through use of the numerical integration mesh. (Note that additional Pulay-like terms are required to calculate accurate forces in computational schemes in which fits are made to the charge density and exchange-correlation energy density. These additional Pulay-like terms account for incompleteness in the basis of fitting functions. See the work of Fournier, Andzelm, and Salahub[20] for a discussion of these techniques.)

The LSDA total energy and the atomic forces are used together in an automated, conjugate-gradient-based optimization scheme to determine the ground-state geometry of the clusters. The optimization procedure starts with an initial guess for the cluster geometry, typically based on bulk bond lengths. The total energy and forces are calculated for the initial configuration and fed into the conjugate gradient routine, which returns a new set of coordinates along the gradient direction in the space of atomic positions. Total energies and forces for successive new configurations are used by the conjugate gradient routine to find the minimum-energy configuration along the given gradient direction, and from that configuration to find the energy minimum along a new conjugate gradient direction, and so on. This process continues until the cluster geometry is fully relaxed (within any symmetry constraints imposed on the cluster geometry) as judged by the vanishing of the forces on the atoms in the cluster. In a typical calculation, the forces on each atom were required to vanish to less than a tolerance of 0.001 a.u. (0.027 eV/bohr) to identify minimum-energy geometries in this procedure.

Our basis sets for the Cu clusters included $8s$-, $7p$-, and $5d$-type atomic orbitals centered on each atom, contracted from a set of 15 even-tempered single Gaussian exponents between $\alpha=226\,878.0$ and $\alpha=0.05$. Adding additional long-range functions to this basis had a negligible effect on the energy of the dimer, lowering its energy by less than 0.01 eV. The basis was therefore deemed adequate for determining equilibrium structures and binding energies.

For metal-atom clusters, there are frequently several electronic states at or near the highest occupied level, the Fermi level E_F, and the choice of how to distribute the electrons among these states to minimize the LSDA total energy is often unclear. As has been shown elsewhere,[21] the lowest-energy solution can correspond to degenerate, fractionally occupied states at E_F. To obtain the lowest-energy solution, and to avoid self-consistency problems associated with accidental degeneracies at E_F, we have adopted[21] a technique for making the energy variational with respect to the occupation numbers of states near E_F.

The reader is referred to Ref. 21 for the details of the procedure. Note that while accidental degeneracies at E_F are not expected to have a large influence on total energies and forces for large systems, where the degenerate states are typically delocalized over the entire cluster, they can be important for small systems, where the states involved are relatively compact. For the carbon dimer, for example, the equilibrium separation changes by 10% depending on choice of f_i's for the two highest-lying states.[21] This is about an order of magnitude greater than the typical accuracy of the LDA in predicting bond lengths.

To calculate the binding energies (i.e., atomization energies) of the clusters, we use the recently developed[14] generalized gradient approximation (GGA) of Perdew and Wang. The GGA makes gradient corrections to the LSDA form of the exchange-correlation potential, and leads to greatly improved binding energies as compared to the LSDA.[22] In this work we apply the GGA perturbatively to the self-consistent LSDA solution for a given cluster. Using the self-consistent LSDA density and its gradients, we construct the GGA total energy. A more rigorous approach would be to calculate the density and its gradients self-consistently within the GGA; however, Fan and Ziegler[23] have shown that the perturbative approach gives essentially the same bond length and binding-energy results as the more rigorous approach for a variety of systems. Although these authors did not explicitly consider transition-metal systems in their study, their results suggest that differences between the perturbative approach and the fully self-consistent approach will be small for Cu clusters, and we adopt the simpler perturbative method in this work.

III. RESULTS

A. Equilibrium structures

Cu clusters of up to five atoms have been studied using the technique described in the preceding section. The equilibrium geometries for the neutral clusters are given in Fig. 1. As can be seen in the figure, all the clusters were found to have planar structures in the ground state. As discussed further below, the nonlinear trimer structure is about 0.3 eV lower in energy than the lowest-energy linear structure. The Cu_4 rhombus is 1.13 eV lower than the optimal tetrahedral structure. (The planar T-shaped structure for Cu_4 was found to lie 0.55 eV above the rhombus.) Similarly, the trapezoidal structure shown in Fig. 1 for the pentamer is 0.05 eV lower in energy than the lowest nonplanar structure, which was found to be a trigonal bipyramid. The rectangular pyramid structure was 0.36 eV above the trapezoid.

By removing an electron from each of the clusters of Fig. 1 and performing self-consistent calculations of the cation cluster total energies, we determined the vertical ionization potentials (IP's) for the clusters. The results are compared with available experimental values[24] for the IP's in Table I. It can be seen in the table that the LSDA results are in reasonable agreement with experiment,

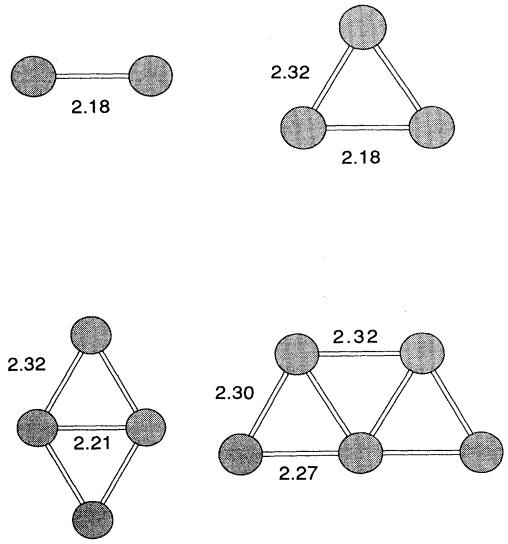

FIG. 1. The equilibrium structures for the neutral Cu clusters with $n \leq 5$. Bond lengths are given in angstroms.

showing clearly the odd–even alternation of ionization energies typical of small metal clusters.

The ground-state neutral clusters all have the lowest possible total spin. Cu_3 and Cu_5 each have a net electron spin of $m_s = \frac{1}{2}$ due to an overall odd number of electrons, while Cu_2 and Cu_4 have zero net spin. Furthermore, the dimer and tetramer had closed-shell electronic structures, with energy gaps of 2.02 and 0.97 eV between the highest occupied and lowest unoccupied states, respectively. The Cu_3 structure has an accidental degeneracy at the Fermi level, which, as discussed further in Sec. III C below, is related to the Jahn-Teller distortion of the equilateral triangle geometry for the trimer.

The planar ground-state structures of Fig. 1 are topologically similar to the minimum-energy structures found for the corresponding alkali-metal clusters,[25] suggesting that the similar electronic structure of the atoms leads to similar bonding in the clusters. Note that group IIa clusters are found to have three-dimensional ground-state geometries for the tetramers and pentamers.[26] The comparison of the present results with corresponding results for alkali-metal clusters is taken up again in Sec. IV below.

TABLE I. Vertical ionization potentials for the neutral Cu clusters.

	LSDA (eV)	Expt.[a] (eV)
Cu	8.43	7.72
Cu_2	8.61	> 6.4
Cu_3	6.30	5.80
Cu_4	7.24	> 6.4
Cu_5	6.80	6.30

[a]Reference 24.

B. Cu_2

In Fig. 2 are plots of the cluster total energy versus separation for the Cu dimer and the dimer anion near their respective minima. The neutral dimer has a minimum-energy separation of 2.18 Å; a polynomial fit of the potential curve yields a vibrational frequency of 292 cm^{-1}. These results are in good agreement with corresponding experimental measurements of 2.22 Å and 265 cm^{-1}.[4] The results also agree well with the earlier $X\alpha$ calculations of Delley *et al.*[9] (2.22 Å and 286 cm^{-1}) and the configuration-interaction (CI) results of Bauschlicher, Walch, and Siegbahn (2.32 Å).[7]

Similarly, the anion curve has a minimum-energy separation of 2.26 Å, and a vibrational frequency of 227 cm^{-1}. These results compare favorably to the experimental values of 2.34 Å and 210 cm^{-1}.[4] Similarly, the calculated cation bond length is 2.29 Å, with a vibrational frequency of 232 cm^{-1}. We are not aware of published experimental values for the cation bond length and vibrational frequency.

The calculated structural properties for both Cu_2 and Cu_2^- are in very good agreement with experiment, and reflect typical accuracies of the LDA for calculating bond lengths and vibrational frequencies. The experimentally observed shift to a larger bond length and softer potential in going from the neutral dimer to the anion is very well reproduced by the calculations. The trend to longer bond lengths and softer potentials in both the anion and cation dimers can be understood on the basis of the electronic structure of the neutral dimer. The neutral dimer is a closed-shell system with a gap of 2.02 eV separating the highest occupied (HOMO) from the lowest unoccupied (LUMO) molecular orbital electronic states. The large gap implies that the HOMO states have considerably more bonding character than the LUMO states. In going to the cation dimer from the neutral, an electron is removed from a bonding HOMO state, resulting in less overall bonding and a longer bond. In the anion dimer, an electron must be added into an antibonding LUMO state, again resulting in weaker bonding and a longer bond.

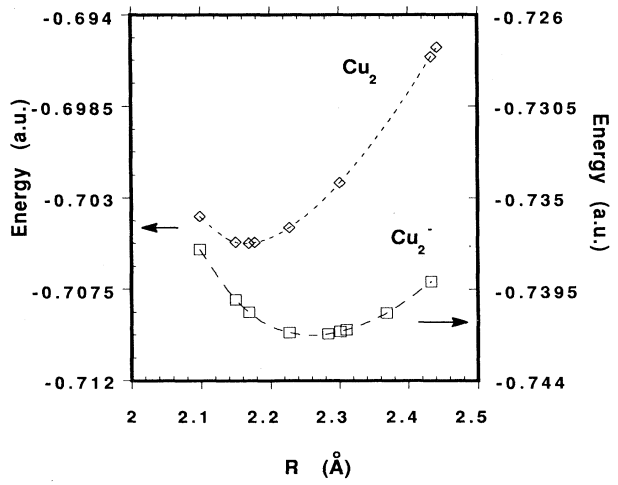

FIG. 2. Total energy vs separation for Cu_2 and Cu_2^-.

TABLE II. Comparison of calculated and experimental results for the Cu dimers.

	LSDA		Expt.[a]	
	r_e (Å)	ω_e (cm^{-1})	r_e (Å)	ω_e (cm^{-1})
Cu_2^+	2.29	232		
Cu_2	2.18	292	2.22	265
Cu_2^-	2.26	227	2.34	210

[a]Reference 4.

By comparing the total energy of the relaxed neutral and anion dimers in Fig. 2, we calculate an adiabatic electron affinity (EA) of 0.97 eV, in good agreement with the experimentally derived value of 0.842 eV.[4] Similarly (though not illustrated in the figure), both the vertical ionization energy, 8.61 eV, and the threshold ionization energy, 8.59 eV, can be determined by taking the appropriate total energy differences.

The results of this section are summarized in Table II.

C. Cu_3

In Fig. 1, the minimum-energy structure for the Cu trimer is shown to be a nearly equilateral triangle, with an average bond length of 2.27 Å. The equilateral triangle geometry has a degenerate electronic ground state. A single electron occupies the twofold degenerate HOMO state. This geometry is thus Jahn-Teller unstable, and distortion to the acute triangle geometry shown in Fig. 1 lowers the energy by 0.02 eV. As mentioned above, the electronic structure of acute triangle Cu_3 geometry has an accidental degeneracy at E_f. The two electronic states (a,b) involved are equivalent by symmetry in the equilateral triangle geometry, and the occupation of the two states is also equal, with $0.5e$ occupying each state. The symmetry is broken by changing the apex angle from 60°, and the two electronic states are no longer equivalent; however, an *accidental* degeneracy of the one-electron energies of a and b persists over a range of apex angles close to 60°. The broken symmetry is reflected instead by the occupation numbers, f_a and f_b. The situation is illustrated in Fig. 3, where the cluster total energy is plotted as a function of apex angle for a fixed triangle perimeter of $P=6.81$ Å. The total energy exhibits a double-well structure, with the acute triangle geometry slightly lower in energy than the obtuse geometry. Included in the figure is the behavior of the occupation number f_a as a function of apex angle. The occupation number of the b state is just $f_b=1-f_a$. From Fig. 3 it is clear that the accidental degeneracy between a and b persists over the range $56° < \theta < 64°$, and f_a varies essentially linearly with the apex angle over this range. In the minimum-energy acute triangle geometry ($\theta \approx 56°$) the occupations are $f_a=0.99$ and $f_b=0.01$.

To illustrate the different character of the two one-electron states a and b, charge-density plots of the two states are shown in Fig. 4. It can be seen that the a state

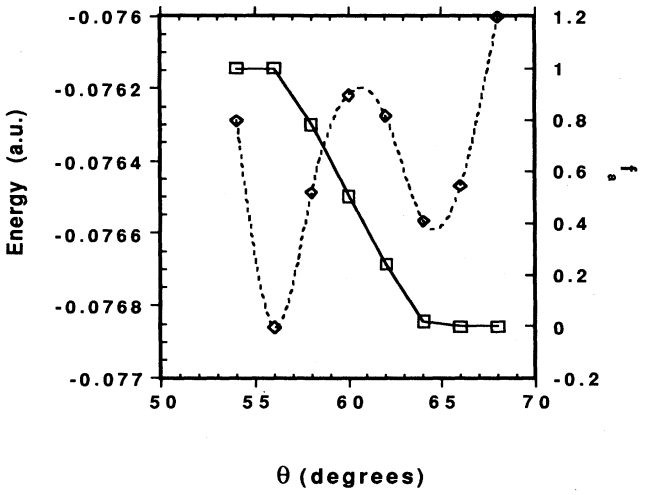

FIG. 3. Total energy (diamonds) and a-state occupation, f_a (squares, see text) vs apex angle for triangular Cu_3 structures. These data correspond to a fixed perimeter of 6.81 Å for the clusters.

concentrates charge density in the region between the two base atoms, enhancing the bonding between these atoms, while the b state places bonding charge density between each of the base atoms and the apex atom. It is clear that shifting charge into the a state will strengthen the bond between the base atoms, leading to the acute triangle structure. Conversely, adding charge to the b state will strengthen the bonds to the apex atom, leading to an obtuse triangle geometry.

The triangular structures for Cu_3 lie about 0.41 eV below the lowest-energy linear configuration (bond length 2.23 Å) of the atoms. The trimer cation Cu_3^+ also has a triangular structure, with an average bond length, 2.24 Å. The linear structure for Cu_3^+ ($a = 2.23$ Å), however, lies 1.85 eV above the nonlinear ground state, a significantly greater energy separation than was seen for the neutral trimers. The increased stabilization of the nonlinear cation structure can be traced to the cation electronic structure. Triangular Cu_3^+ has a stable, closed-shell electronic structure; the linear structure, by contrast, is an open-shell system, with an accidental degeneracy at E_f, and fractionally occupied states.

For Cu_3^- the situation is reversed. In this case, the triangular structure has an open-shell structure, while linear Cu_3^- has a stable, closed-shell structure. Accordingly, we find the linear anion structure to be more stable by 0.56 eV. Note that the triangular anion has a total spin $S = 1$, whereas linear Cu_3^- has total spin $S = 0$.

Walch and Laskowski[8] have performed extensive configuration-interaction (CI) calculations for Cu_3. They also find a double-well energy surface for the neutral trimer, with two nearly degenerate energy minima corresponding to apex angles of 54.9° and 66.9°, respectively. The energy separation between these minima was found to be 0.02 eV, the same separation found here; however, the CI calculation favors the obtuse geometry. Our minimum-energy structure shown in Fig. 1 has an apex angle of 55.9°, which is very close to that of the metastable minimum found by Walch and Laskowski. The lowest-energy linear configuration found in Ref. 8 lies 0.26 eV above the triangular geometries, also in good agreement with the 0.30 eV value given above.

D. Cluster binding energies

The calculated total energies for the Cu atom and Cu^+ and Cu^- can be used with the various cluster total ener-

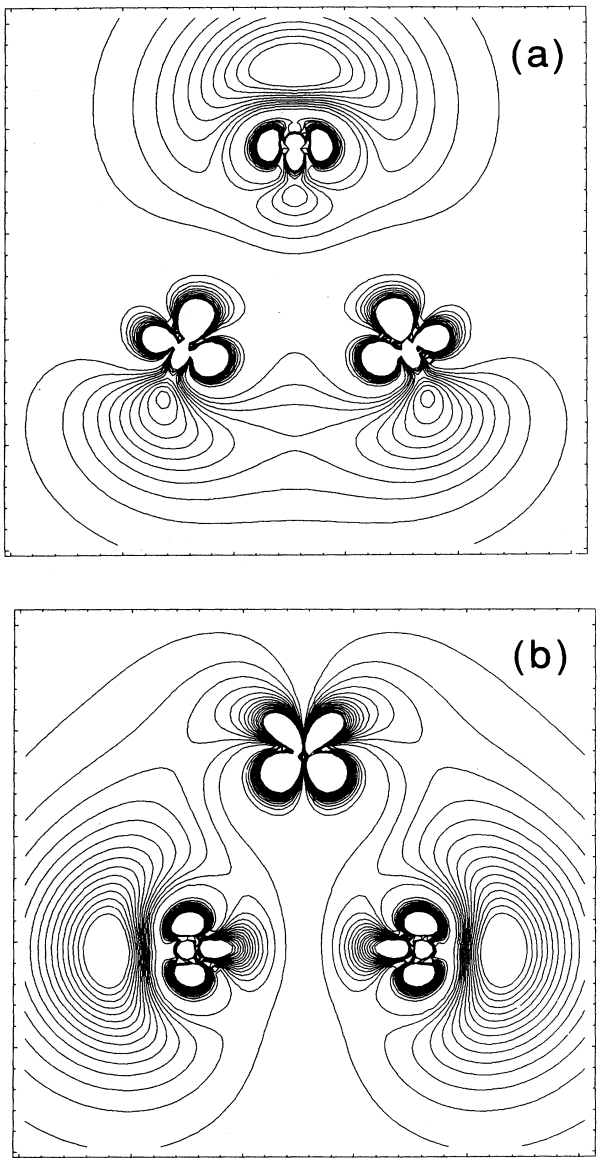

FIG. 4. (a) Charge-density contour plot for the a state (see text) of the minimum-energy Cu_3 structure. (b) Charge-density contour plot for the b state (see text) of the minimum-energy Cu_3 structure.

TABLE III. Cluster binding energies. The values in parentheses give the binding energy per bond in the clusters.

	LSDA (eV)	GGA (eV)	Expt. (eV)
Cu_2	2.72	2.15	2.05
	(2.72)	(2.15)	
Cu_3	4.56	3.47	
	(1.52)	(1.16)	
Cu_4	7.78	6.09	
	(1.56)	(1.22)	
Cu_5	10.48	8.09	
	(1.49)	(1.16)	

gies to calculate the molecular binding energies of the clusters, assuming dissociation into the ground-state atomic species. It is well known, however, that binding energies calculated within the LSDA systematically overestimate experimental binding energies. The Cu_2 cluster binding energies give a direct illustration of this. The calculated LSDA dissociation energy for the neutral dimer is 2.72 eV, compared to a measured value of 1.96 ± 0.06 eV.[4] For Cu_2^-, the calculated value is 2.20 eV, compared to the experimental 1.57 eV.[4] The calculated cation binding energy is 2.57 eV.

The poor LSDA binding energies can be attributed to the local approximation of the exchange correlation energy. Recent gradient-based corrections[14] to the LSDA have shown great promise in improving calculated binding energies. In a series of recent calculations studying hydrocarbon molecules, the generalized gradient approximation (GGA) of Perdew and Wang was found to yield binding energies accurate to within 0.1 eV per bond compared to experiment.[22] By contrast, the LSDA binding energies were accurate to only 0.5 eV per bond.

As discussed in Sec. II, we use the self-consistent charge density and its gradients from the LDA calculation to evaluate the GGA energy functional perturbatively. Using the GGA to calculate the relevant total energies for the dimer and the Cu atom, we find a value of 2.15 eV for the dimer binding energy. This is clearly in much better agreement with experiment than the LDA result. We have used this perturbative GGA approach to calculate the binding energies for the other neutral Cu clusters. The results are presented in Table III.

E. Discussion

As noted in the Introduction, the atomic structure of Cu, $3d^{10}4s$, is similar to that of the alkali-metal atoms, with a single s electron outside closed electronic shells, and it may thus be expected that Cu clusters will share features with alkali-metal clusters of the same size. The ground-state geometries for the neutral Cu clusters shown in Fig. 1, for example, are topologically identical to the corresponding alkali-metal clusters. The proximity of the Cu $3d$ and $4s$ energy levels, however, distinguishes Cu from the alkali-metal atoms, and it is interesting to consider the influence of the $3d$ states on the cluster geometries. A striking feature of Fig. 1 is the recurrence of bond lengths in the various clusters. The dimer bond of 2.18 Å, for example, appears again as the short trimer bond, and (approximately) as the short diagonal in the tetramer. Likewise, the long trimer bond, 2.32 Å, appears as the perimeter bond in the tetramer, and in the pentamer. Also significant is the similarity in different types of bonds in each cluster. In the trimer and tetramer, for example, the short and long bonds differ by less than 6%. This similarity in bond lengths is not seen in the corresponding alkali-metal clusters. For both Li_3 and Na_3, the short bond is nearly 20% shorter than the long bond.[13,14] (Note that these structures are obtuse trian-

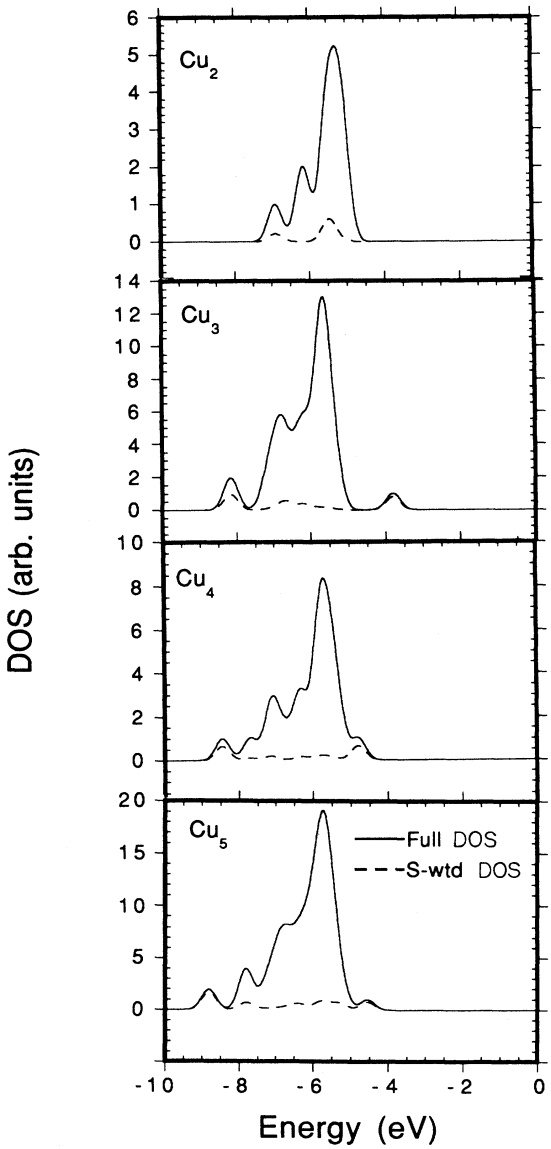

FIG. 5. Valence density of states (DOS) for the neutral Cu clusters with $n \leq 5$. The full lines are the complete DOS; the dotted lines are the DOS weighted by the $4s$ contribution to the cluster eigenstates.

gles, while Cu_3 is acute.) Similarly, the short bond in the Li and Na tetramers are 11% shorter than the long bonds. This comparison shows Cu clusters to have stronger bond-length constraints than either Li or Na clusters, which are themselves very similar. These differences are apparently due to the Cu $3d$ states, and can be understood on the basis of simple bonding arguments. In the alkali metals, shorter bond lengths allow greater overlap of the s orbitals responsible for bonding, and consequently stronger bonds. In the Cu structures, the overlapping $4s$ orbitals must maintain orthogonality to the $3d$ orbitals. This orthogonality constraint represents an added kinetic energy cost to the system for greater overlap, preventing a significant shortening of the bonds. A greater uniformity in cluster bond lengths is the net result.

The role of the Cu $3d$ orbitals in cluster bonding can be illustrated in another way, by examining the d-state character of the cluster valence states. In Fig. 5 we present density of states (DOS) plots for the clusters shown in Fig. 1. These plots are generated using a 0.1-eV Gaussian broadening of the discrete cluster eigenvalues. For each cluster two curves are shown, the first giving the full density of states for the cluster, and the second, dashed curve, showing the density of states weighted by the s-state contribution to each state. This weighting term for the ith electronic state is given by

$$w_i^{(s)} = \sum_{j(s)} \sum_k c_{ij}^{(s)} c_{ik} \langle \phi_j^{(s)} | \phi_k \rangle \ .$$

Here the c_{ij}'s are the eigenvector coefficients for the local orbital ϕ_j in the cluster state Ψ_i. The (s) superscripts indicate that only s-type local orbitals are included in the first summation. The w_i's are simply the Mulliken s-state populations for the cluster eigenstates.

As seen in Fig. 5, there is a strong $4s$ contribution to the states at the bottom and top of the valence manifold. Since these states generally correspond to the most and least bonding electronic states in the clusters, this result is consistent with the view that the $4s$ electrons are important in cluster bonding. The difference between the two curves for each cluster in Fig. 5 represents the $3d$ contribution to the cluster density of states. As can be seen in the figure, there is a significant $3d$ component in the states at the bottom and top of the valence manifold for all the clusters, and particularly for the even-numbered clusters. This implies that there is considerable $3d$-$4s$ hybridization in the electronic states responsible for bonding in the clusters.

Recent theoretical treatments of Cu clusters have been based on one-electron models for the Cu atoms in the clusters.[10,27] It is assumed in these models that the Cu $3d$ orbitals are inert, and that cluster bonding can be explained completely on the basis of the $4s$ electrons alone. The results presented in Fig. 5 suggest that such treatments may miss important effects due to the hybridization of $3d$ and $4s$ orbitals in the cluster bonding states.

IV. CONCLUSIONS

In this work we have reported the results of first-principles LSDA calculations for the structural and electronic properties of small Cu_n clusters with $n \leq 5$. Our calculations of the bond lengths and energy surfaces for Cu_2 and Cu_3 are in good agreement with previous quantum chemical calculations,[7,8,28] and with experimental measurements for these clusters.[4,5,24] In addition, the cluster ionization potentials shown in Table I are in good agreement with experiment.[24]

The calculations show that the small Cu clusters have planar ground-state geometries, similar to the corresponding alkali-metal clusters.[13,14] Unlike the alkali metals, however, the bonds in the individual Cu clusters show small variations in bond lengths, both within a given cluster, and in comparing clusters of different size. This bond-length preference of the clusters was interpreted on the basis of the contribution of the Cu $3d$ states to cluster bonding.

Recent studies[5,10] of Cu clusters have focused on the behavior of cluster properties as a function of cluster size. One facet of this work is to compare predictions of the electronic shell model[29] with observations for the Cu clusters. The shell model has been most usefully applied to explain the properties alkali-metal clusters[30] because of the free-electron-like nature of the s-electrons in the alkali-metal atoms. We have seen in this work that the Cu $3d$ states play an important role in the bonding of the smallest Cu clusters. It can be expected that the participation of the $3d$ states in the cluster bonding will influence the shell model behavior of the clusters. It will be interesting to study larger clusters using the first-principles method described here in order to investigate the role of the d states in the shell model behavior of Cu clusters. Work on larger clusters is currently in progress.

ACKNOWLEDGMENTS

The author would like to thank Dr. Mark R. Pederson for a critical reading of this manuscript before publication. This work was supported by a grant from the Office of Naval Research. Most of the calculations were performed at the Pittsburgh Supercomputer Center.

[1]For a review of the outlook for cluster research in materials science see the DOE panel report by L. E. Brus *et al.*, J. Mater. Res. **4**, 704 (1989).

[2]D. Papaconstantopoulos, *Handbook of the Band Structure of the Elemental Solids* (Plenum, New York, 1986).

[3]C. Kittel, *Introduction to Solid State Physics*, 5th ed. (Wiley, New York, 1976).

[4]D. G. Leopold, J. Ho, and W. C. Lineberger, J. Chem. Phys. **86**, 1715 (1987).

[5]C. L. Pettiette, S. H. Yang, M. J. Craycraft, J. Conceicao, R. T. Laaksonen, O. Cheshnovsky, and R. E. Smalley, J. Chem. Phys. **88**, 5377 (1988).

[6]O. Cheshnovsky, K. J. Taylor, J. Conceicao, and R. E. Smalley, Phys. Rev. Lett. **64**, 1785 (1990).

[7]C. W. Bauschlicher, S. P. Walch, and P. E. M. Siegbahn, J. Chem. Phys. **76**, 6015 (1982).

[8]S. P. Walch and B. C. Laskowski, J. Chem. Phys. **84**, 2734 (1986).
[9]B. Delley, D. E. Ellis, A. J. Freeman, E. J. Baerends, and D. Post, Phys. Rev. B **27**, 2132 (1983); D. Post and E. J. Baerends, Chem. Phys. Lett. **86**, 176 (1982).
[10]O. B. Christensen, K. W. Jacobsen, and J. K. Norskov, Phys. Rev. Lett. **66**, 2219 (1991).
[11]S. Valkealahti and M. Manninen, Phys. Rev. B **45**, 9459 (1992).
[12]P. Hohenberg and W. Kohn, Phys. Rev. **136**, B864 (1964); W. Kohn and L. J. Sham, *ibid.* **140**, A1133 (1965).
[13]R. O. Jones and O. Gunnarson, Rev. Mod. Phys. **61**, 689 (1989).
[14]J. P. Perdew, in *Electronic Structure of Solids '91,* edited by P. Ziesche and H. Eschrig (Akademie Verlag, Berlin, 1991).
[15]J. P. Perdew and A. Zunger, Phys. Rev. B **23**, 5048 (1981).
[16]D. M. Ceperley and B. J. Alder, Phys. Rev. Lett. **45**, 566 (1980).
[17]M. R. Pederson and K. A. Jackson, Phys. Rev. B **41**, 7453 (1990).
[18]K. A. Jackson and M. R. Pederson, Phys. Rev. B **42**, 3276 (1990).
[19]P. Pulay, Mol. Phys. **17**, 197 (1969).
[20]R. Fournier, J. Andzelm, and D. R. Salahub, J. Chem. Phys. **90**, 6371 (1989).
[21]M. R. Pederson and K. A. Jackson, Phys. Rev. B **43**, 7312 (1991).
[22]J. P. Perdew, J. A. Chevary, S. H. Vosko, K. A. Jackson, M. R. Pederson, D. J. Singh, and C. Fiolhais, Phys. Rev. B **46**, 6671 (1992).
[23]L. Fan and T. Ziegler, J. Chem. Phys. **94**, 6057 (1991).
[24]M. Knickelbein, Chem. Phys. Lett. **192**, 129 (1992).
[25]J. L. Martins, J. Buttet, and R. Car, Phys. Rev. B **31**, 1804 (1985); J. Koutecky and P. Fantucci, Chem. Rev. **86**, 539 (1986); B. K. Rao, S. N. Khanna, and P. Jena, Phys. Rev. B **36**, 953 (1987).
[26]F. Reuse, S. N. Khanna, V. de Coulon, and J. Buttet, Phys. Rev. B **41**, 11 743 (1990).
[27]H. Akeby, I. Panas, L. G. M. Pettersen, P. Siegbahn, and U. Wahlgren, J. Phys. Chem. **94**, 5471 (1990).
[28]C. W. Bauschlicher, S. P. Walch, and P. Siegbahn, J. Chem. Phys. **78**, 3347 (1983).
[29]K. Clemenger, Phys. Rev. B **32**, 1359 (1985).
[30]For a review, see W. A. de Heer *et al., Solid State Physics: Advances in Research and Applications,* edited by H. Ehrenreich, F. Seitz, and D. Turnbull (Academic, New York, 1987), Vol. 40, p. 93.